



ISSN 2278 – 0211 (Online)

## A Series Rectifier and NPC Bridge Converter for Large Permanent Magnet Wind Generator Systems

**E. Mahesh**

M.Tech Scholar, EEE Department, NBKRIST, Vidyanagar, India

**S. K. Manjoor Ahamad**

Assistant Professor, EEE Department, NBKRIST, Vidyanagar, India

### Abstract:

This paper proposes a modular, medium voltage, high-power converter topology for the large permanent magnet wind generator system, eliminating the grid-side step-up transformer, which is desirable for both onshore and offshore wind turbines. The converter modules are cascaded to achieve medium voltage output. The power factor correction (PFC) circuit enables the generator to achieve unity power factor operation and the generator armature inductance is used as ac-side PFC boost inductance. The conventional low voltage power conversion system will suffer from a high transmission current, which significantly increases losses and cost of the cables as well as voltage drop. So, in this project a permanent magnet wind generator and high-power converter system is proposed, which increases the converter output voltage by cascading converter modules. The proposed system can reduce the cable losses and associated cost for cables and connections by reducing the current, which provides a solution for the power conversion of large wind turbines. The cascaded Series rectifier and NPC bridge converter can successfully transfer power from the generator to the grid with independent active power and reactive power control ability. The entire proposed system will be tested using MATLAB/SIMULINK and the Simulation results show that the proposed system can successfully operate during system start and power transfer.

**Keywords:** Cascaded H-bridge converter, high-power medium voltage converter, permanent magnet generator, transformerless, wind power

### 1. Introduction

Today a doubly fed induction generator (DFIG) with a partially rated rotor-side converter is the mainstream technology in the market for large wind turbines. Meanwhile, a permanent magnet generator (PMG) interfaced to the grid through a full power converter is increasingly being adopted due to its higher power density, better controllability, and reliability, especially so during grid faults [1]. The voltage level of a wind power converter is usually in the range of 380~690 V due to generator voltage rating and voltage limitation of power electronics devices. Therefore, the power converter is connected to the grid via a step-up transformer to match the grid voltage

WIND TURBINE POWER (MW)	VOLTAGE (KV)	CURRENT (A)
5.0	0.69	4400
	10	303
	35	86
10	0.69	8810
	10	607
	35	173

Table 1: Wind Turbine Current Rating For Different Voltage Levels

Level (10.5 ~ 35 kV) in the wind farm collection system. In the low voltage (690 V) system, when wind turbine power is larger than 500 kVA, several power converters are connected in parallel to handle the increasing current [2]–[6]. The large current transfer also results in a parallel connection of multiple cables and causes substantial losses, voltage drop as well as high cost of cables and connections. This disadvantage can be avoided by placing the step-up transformer into the nacelle. However, the bulky and heavy transformer significantly increases the mechanical stress of the tower. Instead of paralleling converters and cables, another alternative to transfer high power is to use medium voltage transmission, where the current is reduced and the step-up transformer may not be needed if the converter output voltage level can reach the grid voltage (10.5 kV 35 kV) [2], [3]. Hence, a transformer less, medium voltage high power converter system would be an attractive technology for large wind turbines, especially when today's wind turbine power rating is approaching 5 MW and above [4]–[6]. Since the system current rating can be a good indicator for the cable and connection cost and losses, Table I shows the current rating comparison of a 5- and 10-MW system with different voltage levels. As can be seen, the increase of voltage level to 10 or 35 kV can significantly reduce the current ratings.

Medium-voltage high power converters have been widely used for motor drive applications, such as neutral point clamped (NPC) converters and cascaded H-bridge converters, which benefits from multilevel voltage output, less voltage stress, and better harmonic spectrums [7]. The cascaded H-bridge converter is recognized as more suitable for industrial product in the sense of modular structure, high reliability, and fault-tolerant ability. In addition, it is the only available and practical multilevel converter topology that may meet the voltage level of more than 10 kV subject to the voltage rating of power electronic devices. For motor drive applications, the cascaded H-bridge converter needs several independent power sources for the inputs, which are usually provided by an input transformer with multiple secondary windings [8]. Whereas, in a wind power conversion system, the multiple generator coils can be used as the independent sources for the converter modules as shown in figure.

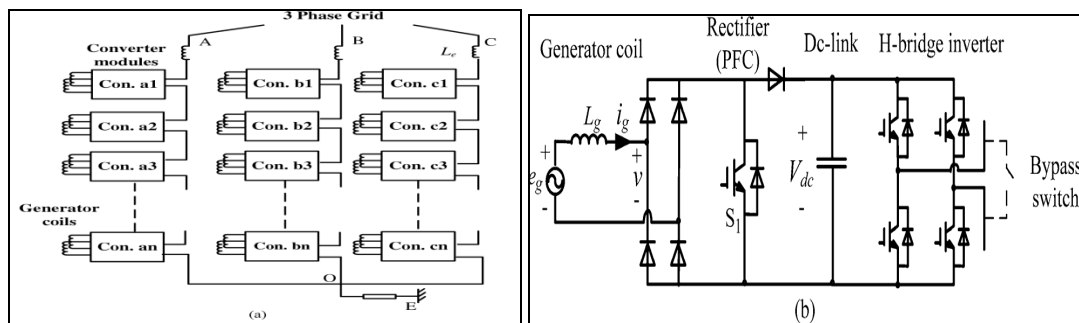


Figure 1: Configuration of the proposed system.

(a) Electrical configuration of the wind generator and multilevel high-power converter system; (b) topology of the converter cell

Based on this, this paper presents a modular permanent magnet wind generator and medium-voltage converter system, aiming to reduce the system current rating by cascading converter modules as shown in Fig.1(a). Each module is composed of a rectifier fed from isolated generator coils, a dc-link, and an H-bridge inverter, as shown in Fig. 1(b).

Previous papers have studied the design of multi pole direct-drive PMG, which has a number of isolated coils [9], [10]. Similar converter topologies are proposed in [11] and [12], without further considering the control and implementation issues, whereas in [2] and [13], the authors mainly focus on the control of the cascaded H-bridge inverters with a staircase modulation.

Unlike the conventional cascaded H-bridge converter used in motor drive applications, the wind power converter serves as the interface between the wind generator and the grid. At the generator side, each converter module requires a stable voltage source input, where a pair of generator coils with  $90^\circ$  phase shift are connected either in parallel or in series to reduce the low frequency power ripple. This will require a special winding arrangement of the generator as well as a control strategy for the generator-side rectifier. A single-switch boost-type power factor correction (PFC) circuit is used as the rectifier, enabling the generator unity power factor operation and also maintaining the converter cell dc-link voltage under different wind speeds. At the grid side, the cascaded H-bridge converter is facing the grid instead of the motor. Then, the control scheme should allow active power and reactive power transferred to the grid as well as dealing with different grid conditions such as grid faults. The voltage oriented vector-control strategy is used to achieve independent control of active power and reactive power fed into the grid and phase-shifted PWM is used for modulating the cascaded converter. The proposed topology and control method is verified by a 2-MW 11-kV grid simulation system and also by a 3-kW experimental system. The paper is organized as follows: Section II describes the basic structure of the generator-converter system and the associated control strategy is developed. The generator design issues regarding winding arrangement and insulation requirement to be compatible with the proposed converter structure are also discussed. Section III presents simulation and experimental results to validate the proposed topology and control method.

## 2. Converter Topology and Control Method

The modular wind power converter system is shown in Fig. 1. As seen, in each phase, several low voltage rating modules (converter cells) are connected in series to achieve medium voltage Output (10.5 ~ 35 kV). Therefore, the converter can be directly connected to the grid via the filter inductance, eliminating the step-up transformer. Each converter cell is composed of an active rectifier, a dc-link, and an H-bridge inverter, as shown in Fig. 1(b). In fact, the active rectifier can take different structures such as full-bridge, half-bridge,

bridgeless converter or single-switch PFC [14]. Since the generator only requires unity power factor operation and the power flow is unidirectional (from generator to the grid), the single-switch type PFC can meet the requirement with the simplest structure and is adopted as in Fig. 1(b).

This circuit has only one active switch that needs to be controlled, which simplifies the control complexity, especially when the number of converter modules is significant. The system neutral point O is grounded via some impedance to improve the system phase to ground fault tolerance and blocking the zero-sequence current [15]. During normal operation, the voltage across the grounding impedance [ $V_{OE}$  in Fig. 1(a)] will be a small portion of the system common-mode (CM) voltage as a result of switching. While during phase to ground fault, the phase voltage will be seen on the impedance, which can be used to detect the ground fault condition.

### 2.1. Converter Cell Topology and Design Considerations

In Fig. 1(b), each isolated generator coil is rectified through a PFC circuit to achieve unity power factor operation and maintain the dc-link voltage of the converter cell under different wind speeds. In addition to the dc component, the output power of a single-phase PFC circuit contains an ac component ( $2\omega_g$ ) with twice the generator stator frequency, as shown in (1)

$$P_{g\_single}(t) = e_g \cdot i_g = E_m \sin(\omega_g t) \cdot I_m \sin(\omega_g t) = (E_m I_m / 2) - (E_m I_m / 2) \cos(2\omega_g t) \quad (1)$$

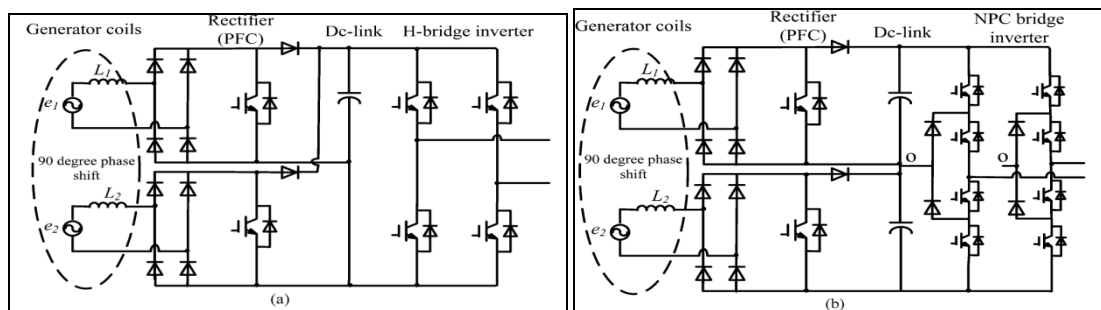


Figure 2: Converter modules with two generator coils of 90 phase shift connected in parallel or in series and the corresponding rectifier and inverter topology. (a) Parallel rectifier and a H-bridge inverter. (b) Series rectifier and an NPC inverter.

Where  $e_g$  and  $i_g$  are the amplitudes of the generator coil back-EMF ( $e_g$ ) and current  $i_g$ , respectively.  $\omega_g$  is the generator stator frequency. This power pulsation with the frequency of  $2\omega_g$  will cause dc-link voltage ripple and affect the H-bridge inverter output. For direct-drive PMG, since the stator frequency  $\omega_g$  is relatively low (usually below 15 Hz), it requires a large dc-link capacitor to reduce the voltage ripple, which significantly increases the system cost. The capacitor lifetime will affect system reliability as well. In this paper, the output of two generator coils with  $90^\circ$  phase shift are rectified and connected either in parallel or in series to cancel out the ac power component, as indicated.

$$\begin{aligned} P_{g\_pair}(t) &= E_{m1} \sin(\omega_g t) I_{m1} \sin(\omega_g t) \\ &+ E_{m2} \sin(\omega_g t + \frac{\pi}{2}) \sqrt{2} I_{m2} \sin(\omega_g t + \frac{\pi}{2}) \\ &= E_{m1} I_{m1} \end{aligned} \quad (2)$$

The ac component of the dc-link power is thus eliminated and the power keeps constant. Accordingly, the converter cell topology will transform from Fig. 1(b) to be as in Fig. 2.

In Fig. 2(a), the two generator coils of  $90^\circ$  phase shift and their PFC circuits are connected in parallel. Therefore, the power from the generator side is constant as shown in (2) and the size of the dc-link capacitor can be reduced. The dc-link capacitor only needs to handle the power ripple from the H-bridge inverter and the high-frequency switching harmonics. Another alternative is to connect the two generator coils in series as shown in Fig. 2(b); this structure can also meet the constant power condition and the dc-link voltage will be twice of the parallel structure as in Fig. 2(a). Correspondingly, the module grid-side inverter can adopt a three-level NPC-type converter to match the dc-link voltage level if the power electronics device of the same voltage rating is used for both rectifier and inverter. An advantage of the structure in Fig. 2(b) is that the dc-link voltage is doubled. Therefore, the grid voltage level can be reached with half the number of modules cascaded compared with the structure in Fig. 2(a), and hence the total number of the independent generator coils required is reduced, which is useful considering the limited number of generator coils and the complexity of winding terminal connection in practice. It should also be noted that, since the neutral point [point O in Fig. 2(b)] in NPC inverter is actively clamped by the front generator-side rectifier, the intrinsic neutral point voltage balancing problem in NPC converter is not a concern here. However, in the series structure, although the whole dc-link power from the generator is constant, the neutral point O still has low frequency ripple ( $2\omega_g$ ) due to (1), which may affect the NPC bridge voltage output to some extent. Since the control strategies for the two types of converter cells in Fig. 2 are similar, this paper will focus on the design and control of the parallel structure in Fig. 2(a).

In the proposed topology, generator armature inductance is used as ac-side boost inductance, as shown in Fig. 2 ( $L_1$  and  $L_2$ ), without requiring extra inductance. The design value of generator armature inductance is mainly determined by the PMG stator current ripple constraint and the current zero-crossing distortion. As observed in Fig. 3, although the coil current reference is sinusoidal, the real coil current will have current ripple and current zero-crossing distortion. The current zero-crossing distortion is an intrinsic problem

associated with the single-switch boost-type PFC circuit, since the polarity of the rectifier voltage [ in Fig. 1(b)] is determined by the coil current direction (which two diodes conduct) [16]. In theory, larger inductance will reduce the current ripple while causing larger current zero-crossing distortion.

The lower limit of generator inductance is then given by the amplitude of the current ripple  $\delta I_m$  as well as the dc-link voltage  $V_{dc}$  and the switching frequency [17], as follows:

$$L_g \geq \frac{V_{dc}}{4\delta I_m f_g} \quad (3)$$

Where  $I_m$  is the peak value of the generator coil sinusoidal current,  $\delta$  and is the factor to determine the allowable current ripple. From (3), smaller current ripple requires larger inductance. On the other hand, the inductance value will affect current zero-crossing distortion. The current distortion angle at zero crossing can be calculated by [17]

$$\alpha = 2 \arctg \left( \frac{\omega_g L_g I_m}{E_m} \right) \quad (4)$$

Where  $E_m$  is the peak value of the generator back EMF. From (4), the larger the inductance is, the larger the zero-crossing distortion angle will be, which affects the current waveform and reduces the generator power factor. Therefore, the upper limit of the inductance should meet

$$L_g \leq \frac{E_m}{\omega_g I_m} t_g \frac{\alpha_{cr}}{2} \quad (5)$$

Where  $\alpha_{cr}$  is the maximum allowable current distortion angle. Hence, the design value of generator inductance should meet (3) and (5) as well as other generator specifications, such as generator short-circuits current.

2.2. Model of Generator-Side Rectifier and Control Strategy

The generator-side rectifier model can be derived from the basic structure in Fig. 1(b), regardless of whether the rectifier is based on the parallel or series structure as shown in Fig. 2. The relationship between coil current, generator back-EMF, and rectifier ac-side voltage (v) is given by

$$e_g = v + L_g \frac{di_g}{dt} \quad (6)$$

Where  $e_g$  is the generator coil back-EMF,  $v$  is the rectifier ac-side voltage, and  $I_g$  and  $L_g$  are the coil current and inductance, respectively. From (6), it can be seen that the coil current  $I_g$  can be controlled by applying appropriate converter voltage, as shown in the simplified circuit diagram in Fig. 4(a). In order to reduce the generator losses, the generator is controlled to be operated under unity power factor. In this case, the coil current is in phase with the generator back-EMF and the phase diagram is shown in Fig. 4(b).

Meanwhile, the rectifier ac-side voltage (v) is determined by the duty cycle of the main switch, (S1) dc-link voltage, and the coil current direction, which is expressed as follows:

$$v = (1 - d) V_{dc} \text{sign}(i_g) \quad (7)$$

Where  $d_n$  is the rectifier main switch duty cycle;  $V_{dc}$  is the dc-link voltage; sign represents the current direction, which will determine which two diodes conduct in the rectifier in

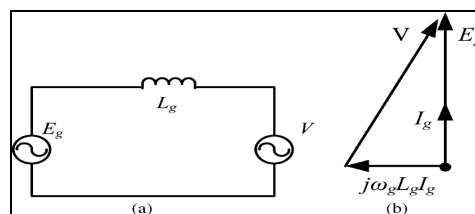


Figure 4: Diagram of the generator-side rectifier. (a) Simplified rectifier circuit diagram; (b) phasor diagram under unity power factor

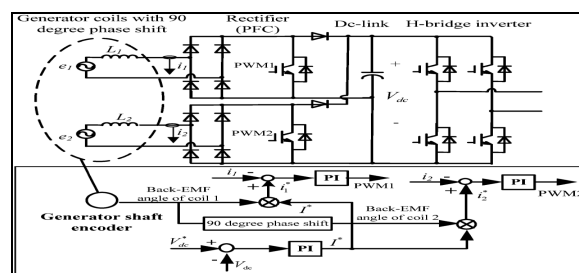


Figure 5: Rectifier control diagram

Fig. 1(b) and the polarity of is then determined accordingly. Based on (6) and (7), the control strategy can be developed, where the current control loop will enable the coil current to track the generator back-EMF to achieve unity power factor operation. For the parallel or series structure in Fig. 2, the two rectifiers can be controlled independently.

The whole control diagram for the paralleled rectifier in Fig. 2(a) is developed as shown in Fig. 5, which has outer dc-link voltage control loop and inner current control loop. The outer loop maintains the dc-link voltage of the converter cell under different wind speeds and its output provides the reference of the current amplitude for the inner current loop. Together with the phase angle of generator back-EMF, the coil current reference can be found. The inner current loop enables the coil current to keep sinusoidal and track the generator back-EMF. Meanwhile, the current loop can also achieve proper power sharing between the two paralleled rectifiers. PI controllers are used here as the outer voltage loop controller as well as inner current loop controller and the proportional and integral gains can be determined by the required control bandwidth and based on the model in (6) and (7). Note that, as shown in the topology in Fig. 5, the generator back-EMF (e1 and e2 ) cannot be measured directly. Therefore, the phase angle of generator coil back-EMF is reconstructed based on the generator rotor position and the distribution of stator coils (angle). The generator rotor position is measured via the shaft encoder as shown in Fig. 5. Once the rotor position is obtained, the phase angle of generator coil back-EMF can be reconstructed based on the stator coil location.

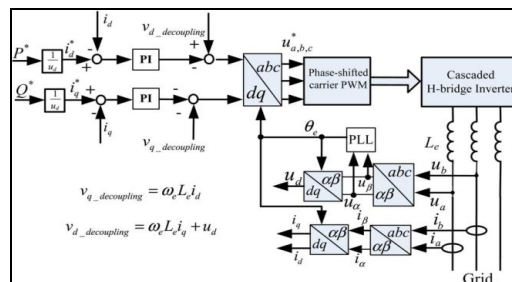


Figure 6: Vector control diagram of the grid-side cascaded H-bridge converter

### 2.3. Model of Grid-Side Cascaded H-Bridge Converter and Control Strategy

At the grid-side, the H-bridge inverters of each converter cell are connected in series to achieve medium voltage multilevel output, interfacing with the grid via the filter inductance as shown in Fig. 1(a). If assuming the dc-link voltage of each series-connected converter cell are the same (the dc-link voltage is regulated by the rectifier), then the cascaded H-bridge converter can be modeled as one voltage source converter and its output voltage is shared equally among the converter cells. Then, the grid-side cascaded H-bridge converter can be modeled in d-q frame, which rotates synchronously with the grid voltage vector, as follows [18]–[20]:

$$\begin{aligned} L_e \frac{di_d}{dt} &= -R_e i_d + \omega_e L_e i_q - S_d + V_d \\ L_e \frac{di_q}{dt} &= -R_e i_q + \omega_e L_e i_d - S_q + V_q \end{aligned} \quad (8)$$

Where  $L_e$  and  $R_e$  are the grid inductance and resistance,  $V_d, V_q, I_d,$  and  $I_q$  are the grid voltages and  $I_q$  currents in the frame, respectively.  $S_d$  and  $S_q$  are the output voltages of the cascaded H-bridge converter along the d-axis and q-axis in the switching average model  $\omega_e$  is the grid line frequency. If the d-axis of the rotating frame is oriented along the grid voltage vector ( $V_q = 0$ ), then the converter active power and reactive power  $Q$  can be formulated by

$$\begin{aligned} P &= v_d i_d + v_q i_q = v_d i_d \\ Q &= v_d i_q + v_q i_d = v_d i_q \end{aligned} \quad (9)$$

From (9), it is shown that the converter output active power and reactive power can be controlled independently by controlling the d-axis and q-axis current. Based on this, the vector control diagram for the grid-side cascaded H-bridge converter is developed as illustrated in Fig. 6 [19], [21]. As seen, the active power and reactive power demand is given as the reference. From (9), the d-axis and q-axis current reference can then be found by dividing the active power and reactive power by the grid-voltage  $V_d$ . The active power demand is usually set based on the wind speed and wind turbine characteristic to achieve maximum power point tracking (MPPT). The reactive power  $Q$  is usually generated to support the grid voltage. The current loop controller adopts the PI controller to control the d-axis and q-axis current independently. The grid voltage angle  $\theta_e$ , which is used for coordinate transformation, can be derived through phase-locked loop (PLL), as described in [22].

In the above analysis, the cascaded H-bridge converter is regarded as a single voltage source converter. The modulation strategy must be developed to modulate the cascaded H-bridge converter once the voltage reference  $V_{a,b,c}$  is obtained from the current loop, as shown in Fig. 6. The modulation of cascaded H-bridge inverter employs the so-called phase-shifted carrier PWM, where the carrier signal of each cascaded converter cell has a phase shift with each other by a certain degree and is compared with the common modulation signal. This modulation scheme can enable the converter to achieve multilevel voltage output when several converter cells are connected in series. It can also guarantee the equal power sharing between the cascaded cells, since the output voltage of each cell is the same (only has a small phase shift) and the current is the same (because they are in series). Fig. 7 illustrates the modulation scheme with three stages of H-bridge inverter cells in series. Fig. 7(a) shows the modulation signals (obtained from current

loop output) for the first-stage H-bridge inverter, which are compared with the carrier signal to get gate signal of the left and right phase leg of the H-bridge cell. Note that, the two modulation signals are out of phase with each other so that the output voltage of H-bridge cell has a unipolar (three-level) output as shown in Fig. 7(b). Similarly, the other two stages are modulated with the same modulation signal as in Fig. 7(a), but with phase-shifted carrier signals as in Fig. 7(c). Subsequently, the output voltage of the cascaded H-bridge cells (three stages) has seven voltage levels, which optimizes the harmonics due to the switching.

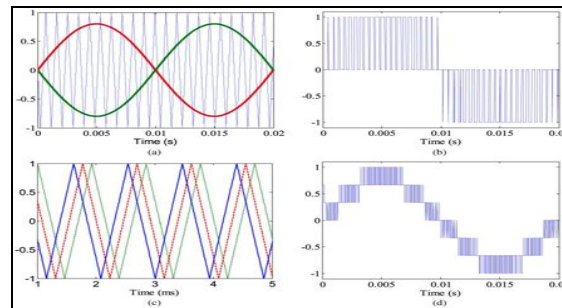


Figure 7: Illustration of the modulation scheme of cascaded H-bridge inverter. (a) Modulation of one H-bridge inverter; (b) output voltage of one H-bridge inverter; (c) carrier signals of three-stages H-bridge inverters; (d) output voltage of the cascaded H-bridge inverter with three stages (seven levels).

Modulated with the same modulation signal as in Fig. 7(a), but with phase-shifted carrier signals as in Fig. 7(c). Subsequently, the output voltage of the cascaded H-bridge cells (three stages) has seven voltage levels, which optimizes the harmonics due to the switching.

It should also be noted that, besides the dc component, the output power of each H-bridge inverter cell contains power ripple as well, and its frequency is twice of the fundamental output voltage frequency (the same as grid frequency in this case). However, the power ripple frequency here is much higher than the one from the generator side. The ripple frequency is 100 Hz for a 50-Hz grid and 120 Hz for a 60-Hz grid. Therefore, it may be filtered with a relatively smaller dc-link capacitor.

#### 2.4. Generator Design Considerations

The wind generator must be designed to be compatible with the converter topology in terms of stator winding arrangement, insulation requirement, and so on. As shown in Fig. 2, every converter cell needs a pair of generator coils with  $90^\circ$  phase shift. The conventional three-phase generator may not meet this requirement. Hence, the multiphase (more than three phases) generator is used to achieve the required phase shift between different coils. Fig. 8 presents the stator winding diagram of a six-phase six-pole PMG (dual three phase windings,  $30^\circ$  phase shift). As seen, there are a number of coils with  $90^\circ$  phase shift, depending on the number of poles of the generator, which is quite a few for direct-drive PMG. In practice, coils of the same phase (belonging to different poles) can be connected flexibly, either in series or connected out separately to meet the application needs, for example, to meet the voltage rating requirement of each cell. Note that, besides the six-phase generator, the PMGs with multiples of six phases (i.e., 12, 18, 24) will also have coil pairs with  $90^\circ$  phase shifts.

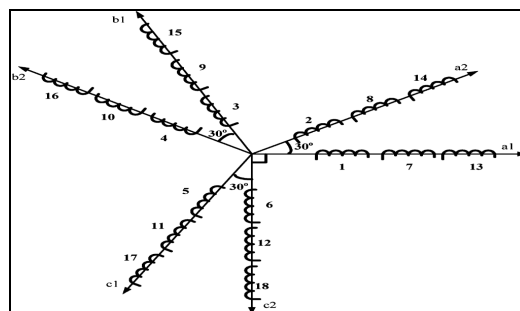


Figure 8: Stator winding diagram of a six-phase PMG

The use of a multiphase generator also benefits from fault-tolerant ability and reduced torque ripple [23]. Taking the six-phase generator shown in Fig. 8 for example, the third, fifth, seventh order harmonics in the generator back-EMF will not cause the low-frequency torque ripple. The lowest order of torque ripple will be 12th order, caused by 11th and 13th harmonics interaction with the sinusoidal current. In the proposed topology, the generator insulation should withstand grid voltage level (10 33 kV) due to the elimination of the step-up transformer. The insulation issues may be a challenge in the generator design. Generators which operate on these voltage levels are commonly made of form-wound coils covered with three insulation layers: strand insulation, turn insulation, and ground-wall insulation (insulation between coil and the stator core). The ground-wall insulation is imposed to the highest voltage stress at end winding terminal, which corresponds to ground voltage. Also, semi-conductive coating and ripple springs are used to

eliminate the possibility for external partial discharges (corona) caused by air voids between ground-wall insulation and a stator core [5].

### 2.5. System Level Operation Strategy and Fault Tolerant Discussion

In this section, application issues such as system start, MPPT operation, grid integration, and fault tolerant ability are discussed. The starting process of the wind generator and converter system is designed as follows: when the wind speed reaches cut-in speed [21], the generator-side converter starts to operate and maintains the dc-link voltage at the reference value. Once the dc-link voltage is built up, the grid-side contactor [not shown in Fig. 1(a)] closes to connect the cascaded H-bridge converter to the grid. Since the equivalent dc-link voltage of the series connected converter cells are set higher than the grid phase voltage, as a result, there will be no inrush current when the converter is connected to the grid. Then, the grid-side cascaded H-bridge

Converter starts to operate, controlling the active power and reactive power fed into the grid with the control diagram as shown in Fig. 6. To achieve MPPT, the active power reference of the grid-side cascaded H-bridge converter is set based on the present wind speed and also the wind turbine characteristics to allow maximum power delivery. Meanwhile, the generator-side rectifier monitors and maintains the dc-link voltage of the converter cell. Subsequently, the generator is adjusting its power output to track the active power reference at the grid-side converter, thus achieving MPPT.

One advantage of using the modular structure of the power converter is that the system may still maintain continuous operation (the output power may reduce) if one of the converter cells fails. For example, if one of the main switches fails in the H-bridge inverter cell, the failure H-bridge inverter can be bypassed by an extra switch (e.g., thyristor) which is connected in parallel with the output of the converter cell as shown in Fig. 1(b)[24], [25]. In this case, the rest of the healthy cells may need to increase their dc-link voltages to meet the grid voltage level and continue operation. The module failure may also cause the imbalance of the generator, where the level of impact depends on the multiphase generator design. Since the proposed converter is facing the grid, the system should also be able to handle grid faults, such as voltage dip and unbalance, which may be a challenge in the practical system. The control strategies for riding through the grid faults used in two-level full power converters might be adopted and adjusted for the proposed structure [18], [26]. For example, a dump resistor bank might be needed to handle the deep voltage drop. A PLL and advanced current controller which may track the positive sequence voltage/current might be used to manage the grid unbalance.

Grid voltage	11kv	Converter cell DC-link voltage	1400V
Grid Frequency	50 Hz	Number of Converter stages	8
Wind Turbine Power	2MW	Rectifier Switching frequency	8KHz
Number of generator coils	48	H-Bridge inverter Switching frequency	12KHz
Generator coil Rated voltage	848V	Generator side Inductance	900 $\mu$ H
Generator coil Rated Current	48A	Dc-link Capacitor	8000 $\mu$ F
Generator coil Inductance	10mH		

Table 2: Generator and Converter Parameters in the Simulation

## 3. Simulation and Experimental Verification

### 3.1. Simulation Verification

The simulation model for a 2-MW generator and converter system and 11-kV grid is built in MATLAB/Simulink to verify the proposed topology and control method. In the simulation, the PMG has 48 coils, which can form 24 pairs of coils with 90 phase shift. Therefore, the three-phase cascaded converter has eight stages and can output 17 voltage levels. The dc-link voltage of each converter module is set at 1400 V to meet the grid voltage of 11 kV. Based on the generator inductance design rules given in (3) and (5), the generator inductance is chosen to be 10 mH to limit the current ripple within 10% of the maximum current and no more than 10 for the current zero-crossing distortion. Meanwhile, the dc-link capacitor is chosen to be 8000 F to reduce the dc-link voltage ripple (caused by H-bridge inverter power ripple) to be within 1% of the nominal dc-link voltage. The NPC bridge inverter is shown in Fig 16, the dc-link voltage doubles in NPC inverter. The complete parameters for the simulation system are listed in Table II.

The simulation results are shown in Fig. 9. Once the wind speed reaches cut-in speed and the dc-link voltage is regulated to 1400 V, the grid-side contactor will close and the cascaded H-bridge converter starts to operate and control the active and reactive power fed into the grid. Fig. 10 shows the grid current. Fig. 11 shows the grid voltage. Fig. 12 presents the DC link voltage. Fig. 13(a) and (b) shows the grid output voltage and current waveform at UPF. Fig. 14 shows the back emf and current. Fig. 15(a) and (b) show grid voltage and current at fault condition. Fig. 16 shows NPC bridge inverter. Fig. 17 shows DC link voltage, Fig. 18 shows grid voltage. Fig. 19 shows grid current.

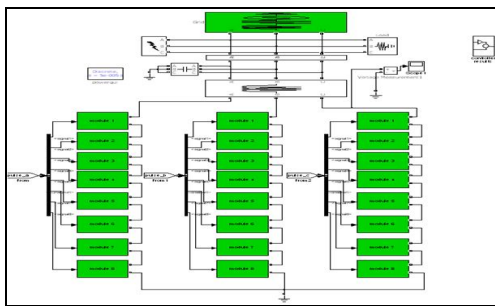


Figure 9: Simulink model

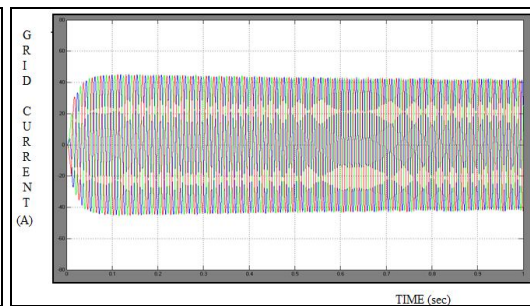


Figure 10: Grid current

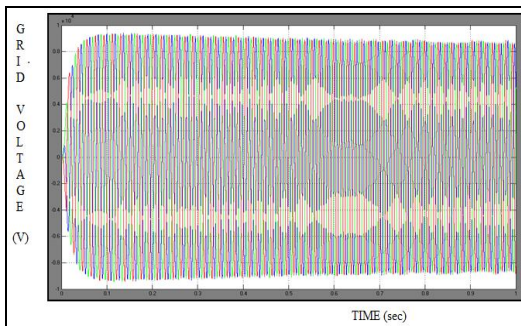


Figure 11: Grid Voltage

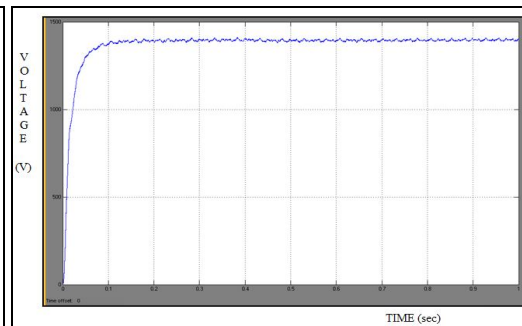


Figure 12: Dc-link Voltage

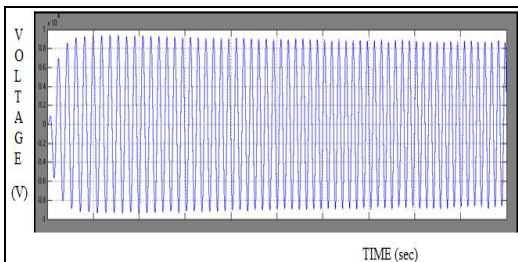


Figure 13(a): Voltage at UPF

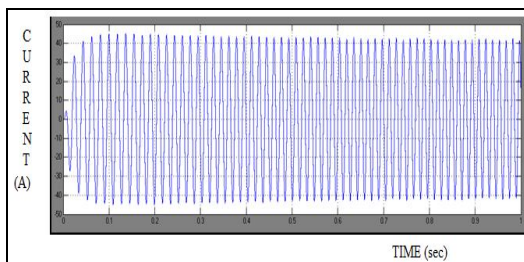


Figure 13(b): Current at UPF

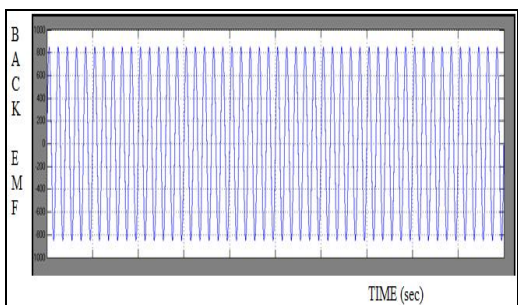


Figure 14(a): Back EMF and current

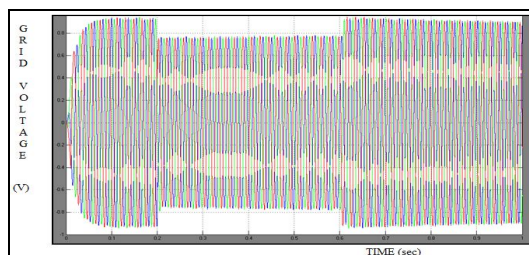
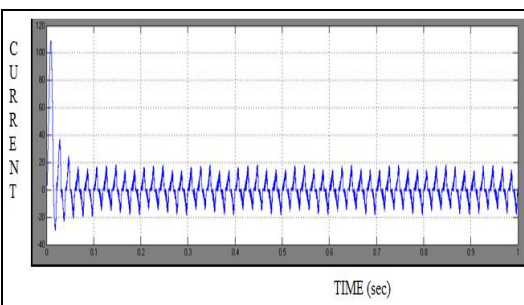


Figure 15(a): Grid voltage under fault

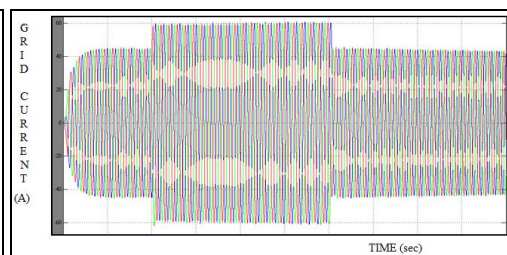


Figure 15(b): Grid current under fault

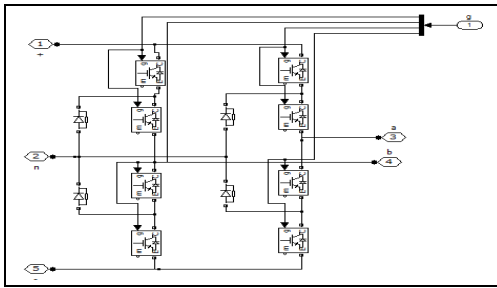


Figure 16: NPC inverter

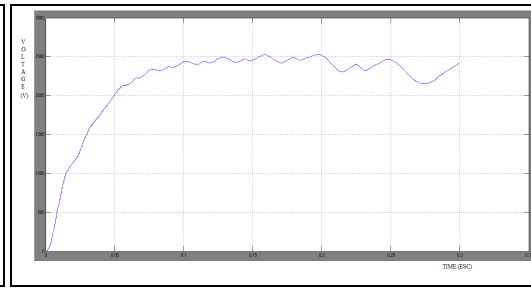


Figure 17: DC- link voltage

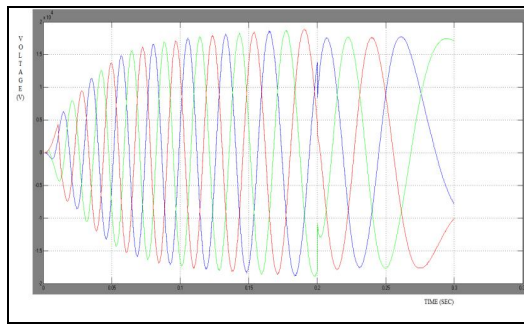


Figure 18: grid voltage

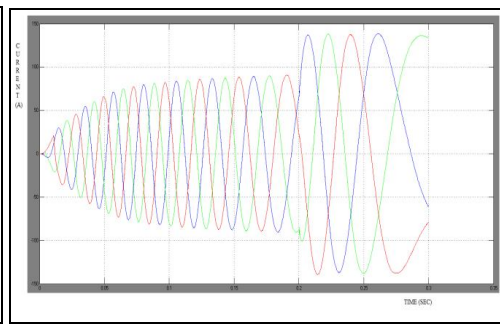


Figure 19: grid current

#### 4. Conclusion

This paper has discussed the way to improve the dc-link voltage of each converter cell in order to reduce the required number of generator coils, thus reducing the converter stages to match the grid voltage level. Here H-bridge inverter and NPC inverter are compared. The phase shifted PWM method is implemented for modulating the H-bridge type converter and NPC inverter. The NPC inverter transfers power double than the H-bridge inverter so the converter modules are less compare to H-bridge inverter. This allows balancing of the power circulating between phases and reduces significantly the size of intermediate capacitors. Moreover, they use less power devices and their control is easier. The proposed system can reduce the cable losses and associated cost for cables and connections by reducing the current, which provides a solution for the power conversion of large wind turbines. The generator coils with 90 phase shift are connected via rectifier either in parallel or in series to achieve a constant dc-link power.

#### 5. References

1. F. Blaabjerg and Z. Chen, Power Electronics for Modern Wind Turbines. U.S.: Morgan & Claypool Publishers, 2006, ch. 4.
2. C. Ng, M. Parker, and P. Tavnar, "A multilevel modular converter for a large light weight wind turbine generator," IEEE Trans. Power Electron., vol. 23, no. 3, pp. 1062–1074, May 2008.
3. H. Li and Z. Chen, "Design optimization and evaluation of different wind generator systems," in Proc. IEEE ICEMS'08 Conf., Oct. 2008, vol. 2, pp. 2396–2401.
4. A. Faulstich, J.K Stinke, and F. Wittwer, "Medium voltage converter for permanent magnet wind power generators up to 7 MW," in Proc.EPE Conf., Sep. 2009, pp. 9–17.
5. M. Szykiel, "Overview of power converter designs feasible for high voltage transformer-less wind turbines," in Proc. IEEE ISIE 2011 Conf., Jun. 2011, pp. 1420–1425.
6. K. Ma and F. Blaabjerg, "Multilevel converters for 10 MW wind turbines," in Proc. Eur. Power Electronics Conf., Aug. 2011, pp. 1–7.
7. R. C. Portillo, M.M. Prats, and J. I. Leon et al., "Modeling strategy for back-to-back three-level converters applied to high-power wind turbines," IEEE Trans. Ind. Electron., vol. 53, no. 5, pp. 1483–1491, Oct. 2006.
8. B.Wu, High Power Converters and AC Drives. Hoboken, NJ:Wiley-IEEE Press, 2006.
9. E. Spooner, P. Gordon, and C.D. French, "Lightweight, ironless-stator, PM generators for direct-drive wind turbines," in Proc. Int. Power Electronics, Machines and Drives Conf., Mar. 2004, vol. 1, pp. 29–33.
10. D. Vizireanu, X. Kestelyn, and S. Brisset, "Polyphased modular directdrive wind turbine generator," in Proc. EPE'05 Conf., Sep. 2005, vol. 1, pp. 1–9.
11. J. M. Carrasco, L.G. Franquelo, and J.T. Bialasiewicz, "Power-electronic systems for the grid integration of renewable energy sources: A survey," IEEE Trans. Ind. Electron., vol. 53, no. 4, pp. 1002–1016, Aug. 2006.
12. F. Blaabjerg, F. Iov, T. Terekes, and R. Teodorescu, "Power electronics- key technology 1for renewable energy systems," in Proc. Power Electronics, Drive Systems and Technologies Conf., Feb. 2011, pp. 445–466.
13. M.A. Parker, C.H. Ng, and L. Ran, "Power control of direct drive wind turbine with simplified conversion stage & transformerless grid interface," in Proc. 41st Int. Univ. Power Eng. Conf., Sep. 2006, vol. 2, pp. 65–68.

14. Y. Lo, S. Ou, and H. Chiu, "On evaluating the current distortion of the single-phase switch-mode rectifiers with current slop maps," *IEEE Trans. Ind. Electron.*, vol. 49, no. 5, pp. 1128–1137, Oct. 2002.
15. F. Wang, R. Lai, and X. Yuan, "Failure-mode analysis and protection of three-level neutral-point-clamped PWM voltage source converters," *IEEE Trans. Ind. Appl.*, vol. 46, no. 2, pp. 866–874, Mar. 2010.
16. X. Yuan, Y. Li, and J. Chai, "A transformer-less modular permanent magnet wind generator system with minimum generator coils," in *Proc. IEEE APEC'2010 Conf.*, Feb. 2010, pp. 21–25.
17. L. Liu, Y. Ma, J. Chai, and X. Sun, "Cascaded single phase PFC rectifier pair for permanent magnet wind generation system," in *Proc. IEEE IPEMC'08 Conf.*, Oct. 2008, vol. 1, pp. 2516–2520.
18. A. Mullaney, G. Lightbody, and R. Yacamini, "Wind turbine fault ride through enhancement," *IEEE Trans. Power Electron.*, vol. 20, no. 4, pp. 1929–1937, Nov. 2005.
19. X. Liu, P. Wang, and P. Loh, "A hybrid AC/DC microgrid and its coordination control," *IEEE Trans. Smart Grid*, vol. 2, no. 2, pp. 278–286, Jun. 2011.
20. X. Yuan, Y. Li, and J. Chai, "A modular direct-drive permanent magnet wind generator system eliminating the grid-side transformer," in *Proc. Eur. Power Electronics Conf.*, Sep. 2009, pp. 1–7.
21. M. Chinchilla, S. Arnaltes, and J. Burgos, "Control of permanent-magnet generators applied to variable speed wind energy systems connected to the grid," *IEEE Trans. Energy Convers.*, vol. 21, no. 1, pp. 130–135, Mar. 2006.
22. V. Kaura and V. Blasko, "Operation of a phase locked loop system under distorted utility conditions," *IEEE Trans. Ind. Appl.*, vol. 33, no. 1, pp. 58–63, Jan. 1997.
23. K.S. Khan, W.M. Arshad, and S. Kanerva, "On performance figures of multiphase machines," in *Proc. ICEM'08 Conf.*, Sep. 2008, vol. 1, pp. 1–5.
24. J. Rodriguez, S. Bernet, and B. Wu et al., "Multilevel voltage-source converter topologies for industrial medium-voltage drives," *IEEE Trans. Ind. Electron.*, vol. 54, no. 6, pp. 2930–2945, Dec. 2007.
25. M.A. Parker, Ng. Chong, and Ran Li, "Fault-tolerant control for a modular generator converter scheme for direct drive wind turbines," *IEEE Trans. Ind. Electron.*, vol. 58, no. 1, pp. 305–315, Jan. 2011.
26. V. Akhmatov, "Modelling and ride-through capability of variable speed wind turbines with permanent magnet generators," *Wind Energy*, vol. 9, pp. 313–326, Sep. 2006.